Determination of cytotoxicity, biological effects and anti-human breast cancer properties of Bilobol

ALSALEEM MOHAMMED ABADI[1], MOHAMED SAMIR AHMED ZAKI[2,3], ABULQASIM M. SIDEEG[4], ATTALLA F. EL-KOTT[5,6], XIANGYU GUO[7*]

[1]Department of Family and Community Medicine, College of medicine, King Khalid university

[2]Department of Anatomy,College of Medicine, King Khalid University, P.O. 61421, Abha, Saudi Arabia.

[3]Department of Histology and Cell Biology, College of Medicine, Zagazig University, Zagazig 31527, Egypt

[4]Department of Anatomy, College of Medicine, King Khalid University, P.O. 61421, Abha, Saudi Arabia.

[5]Department of Biology, College of Science, King Khalid University, Abha 61421, Saudi Arabia

[6]Department of Zoology, College of Science, Damanhour University, Damanhour, Egypt

[7]Institute of Oncology, Cancer Hospital of Dalian University of Technology, Liaoning Cancer Hospital and Institute, Shenyang, 110042, China.

*Corresponding Author：Dr. Xiangyu Guo, Cancer Hospital of Dalian University of Technology.

Email: gxy18509861568@sina.com,

ORCID: 0000-0002-5912-4513

ABSTRACT

The current research used Bilobol to determine the cytotoxicity and anti-human breast cancer properties with molecular docking studies. The properties of Bilobol against breast cell lines i.e. Hs578T, MDA-MB-231, SkBr3, BT-549, MCF-7, AU565, 600MPE, and Evsa-T were evaluated in the in vitro condition. The IC50 of the Bilobol was 258, 236, 161, 265, 250, 183, 256, and 233 µM against MDA-MB-231, Hs578T, SkBr3, BT-549, MCF-7, AU565, Evsa-T, and 600MPE, respectively. The molecular modeling evaluation analyzed the chemical effects of bilobol against alpha-amylase and alpha-glucosidase. The anti-cancer activities of the molecules were examined against MDA-MB-231, Hs578T, SkBr3, BT-549, MCF-7, AU565, Evsa-T, and 600MPE cell lines. Following completion of clinical trial research, the novel compound may find application in human supplementation against breast cancer. Bilobol's IC50 values for the enzymes α-amylase and α-glucosidase were found to be 45.13 and 11.82 µM, respectively. In the aforementioned cell lines, bilobol's chemical interactions with a few expressed surface receptor proteins (EGFR, CD47, androgen receptor, folate receptor, HER2, CD44, progesterone receptor, and estrogen receptor) were determined using molecular modeling calculations. The outcomes displayed the likely atomic-level interactions and their properties. According to the docking scores, this chemical has a high affinity for certain proteins and enzymes. Additionally, this substance made strong contact with the receptors and enzymes. As a result, both enzymes and cancer cells may be inhibited by this chemical molecule.

Keywords: *Breast cancer; Bilobol; Cell viability; Molecular docking; MTT assay.*

INTRODUCTION

The anticancer impact of the traditional Chinese medicine component bilobol is still unknown. The aim of the current study was to show that bilobol inhibits the growth of breast carcinoma to provide the groundwork for future investigations into the mechanisms underlying this anticancer activity. Bilobol is a substance that is present in cashew nutshell liquid, which comes from the *Anacardium occidentale* (Anacardiaceae) plant. It may be cheaply and efficiently extracted from agricultural waste using a few straightforward processes [1].

Biological molecules have many medical applications, and their usage in conjunction with anticancer medications is becoming more and more common these days. Combining biological molecules with anticancer medications can increase the drug's delivery to the cell and reduce its toxicity to healthy cells, which is one of the practical uses of biological molecules [2]. Modern methods of cancer control and cure are needed because cancer-related deaths are becoming more common and because chemotherapy and radiation treatments have flaws when the disease reaches an advanced stage. Priority one for study is biological molecules with a diameter of 100 nm or smaller that are supplemented with anti-cancer agents to aim cancer cells in cancer studies [3-6]. There is evidence of a strong correlation between the size of biological molecules and their cytotoxic properties. Research demonstrates that there are two ways in which biological molecules kill cancer cells [7-9]. One is the production of cell death through direct interaction or influence on cell structures and cell components (DNA, RNA, and protein). Secondly, they indirectly produce harmful oxygen radicals that eventually encourage cell death [10,11].

The right substrate or biomolecules must be arranged for the proteins in the body to perform their purpose [12]. Biologists can obtain crucial information by determining the interaction between the substrate and related proteins. Since the process of developing new drugs takes a lot of time, computational approaches can help speed up this process [13]. One flexible assay that can provide these data and be applied to the discovery of enzyme substrates is molecular docking analysis. Molecular docking calculations also provide the easily attainable function of evaluating empirical results [14]. Using this method can reveal potential atomic-level interactions between the biomolecules [15]. Molecular docking studies have garnered significant attention as a computer-assisted of drug design method in recent times. Determining therapeutic targets and comprehending biological processes may also facilitate the development of new medications.

Diabetes mellitus is one of the biggest subjects facing science in the twenty-first century. It's a well-known multifactorial health concern that raises mortality rates by causing major health issues, especially those related to renal impairment, cardiovascular disease, and neuropathy [16]. Inhibiting the enzyme α-glucosidase, which catalyzes the hydrolysis action of starch molecule in the intestine, is an efficient treatment method for managing the hyperglycemia brought on by type-2 diabetes. One of the important enzymes in the digestion of carbohydrates is -amylase, which does so by catalyzing the hydrolysis of

the -D-1,4-glucosidic link in starch. Therefore, it is thought that inhibiting α-amylase activity is a good way to control blood sugar levels and treat food-related hyperglycemia [17]. Currently, scientists are thinking about using α-amylase inhibitors in the diet to assist control of hyperglycemia. Therefore, a significant new avenue for the current food and medicine industry could be the search for bioactive substances that are anti α-amylase [18]. In this study, the characteristics of Bilobol against human breast cancer cells i.e. Hs578T, MDA-MB-231, SkBr3, BT-549, MCF-7, AU565, 600MPE, and Evsa-T were assessed and then in the *in vitro* condition bioactivity and in silico effects of it were investigated.

MATERIALS AND METHODS

Measurement of anti-breast cancer properties

Using the MTT colorimetric method, cytotoxic characteristics of bilobol were investigated on breast cancer cells, specifically MDA-MB-231, Hs578T, SkBr3, BT-549, MCF-7, AU565, Evsa-T, and 600MPE. The culture media employed for the cancer cell cultivation was 10% Roswell Park Memorial Institute (RPMI). To make the full culture medium, 90 cc of pre-made RPMI culture media were mixed with 10% RPMI, 10 mL Fetal Bovine Serum, (FBS) and 1 mL each of streptomycin and penicillin. After being taken out of the incubator, the vial holding the cancer cells was placed in Bain-Marie. After that, the Falcon's contents were centrifuged after the contents of the vial and around 5 cc of the culture medium were combined. The cell plate was filled with 1 mL of growth media and the supernatant. After that, the cells were moved into a flask with 5 cc of growth medium, and the flasks were put in a CO_2 incubator that had the right temperature and humidity. The cells were passaged and moved to a new culture medium regularly. After that, the flasks' liquid solution was taken out. The flask's bottom was then cleaned with PBS. Trypsin was added to detach the cells from the plate bottom. Trypan blue dye was used to count the cells, and once the cells had been transferred to a plate, the MTT test was conducted and the plate was then placed in an incubator. The idea behind the discovery is that curmazan is not generated and stays colorless in dead cells because they lack the succinate dehydrogenase enzyme, which combines with tetrazolium in living cells' mitochondrial membrane to produce purple crystals. The process involved cultivating cancer cells in a 96-well plate using RPMI culture media after they were taken from the cell bank. Treatment with Bilobol in multiple dilations (1-1000 µg/mL) was carried out after 24 hours. Afterward wells were filled with 20 µl MTT solution, and the plates were incubated for approximately 4 hours at 37 °C [19]: % Total viable cells in each milliliter of an aliquot is known as viable cells. Total number of cells in an aliquot × 100 milliliters.

Molecular docking study

In this study, two enzymes were used: α-glucosidase (PDB ID: 5KZX) and pancreatic alpha amylase (PDB ID: 1HNY). A number of breast cancer cell lines, including Hs578T, MDA-MB-231, SkBr3, BT-549, MCF-7, AU565, Evsa-T, and 600MPE cell lines, were used to evaluate bilobol's anti-cancer activity because several synthetic and natural chemicals have been demonstrated to have a variety of advantages, including anti-cancer properties [20–22]. We also evaluated the surface receptors that showed high expression in the previously stated cell lines using molecular modeling. For SK-BR-3 [23], EGFR (PDB ID: 5WB7) [24] was selected for MDA-MB-231 [25], androgen receptor (PDB ID: 2Q7I) was selected for MCF-7 [26-28], folate receptor (PDB ID: 4LRH) was selected for Hs578T [29], progesterone receptor (PDB ID: 1A28) was selected for Evsa-T [30], CD44 (PDB ID: 4PZ3) [31] was selected for BT-549 [32], HER2 (PDB ID: 1N8Z) [33] was selected for AU565 [34], and estrogen receptor (PDB ID: 3OS8) was selected for 600MPE cells [35]. Bilobol's chemical activities were measured with these proteins and enzymes. The structures, which came from the PDB database, were produced using the Schrödinger Suite's protein production module (http://www.rcsb.org/pdb) [36]. An H-bond network was created, water molecules were removed, and hydrogen atoms were added to create the structures [37-39]. Schrödinger's SiteMap [40] was utilized to determine the structures' active location. A receptor grid was constructed around the expected active location to ensure a reliable outcome. Schrödinger's LigPrep module was utilized to synthesis the compounds, which were then obtained from the PubChem database [41,42].

Enzymes part

Using p-NPG molecule as the substrate molecule, the inhibitory impacts of the natural chemical on α-glycosidase enzyme were evaluated by the methodology outlined by Tao et al. [43]. Four milligrams and four milliliters were combined to generate the sample (EtOH:H_2O). In the event that complete enzyme inhibition was needed, several phosphate buffer (PB) solutions were prepared. 5 µL of the sample was added after combining 20 µL of the enzyme solution in PB (0.15 U/mL, pH 7.4) with 75 µL of PB. After that, the reaction was begun and pre-incubated for 10 minutes at 37 °C before p-NPG was added. After the preincubation period, 50 µL of p-NPG molecule in phosphate buffer was used, and then it was then incubated at 37 °C once more. At 405 nm, with using spectrophotometry (CAS Number: 9001-42-7, α-Glucosidase from *Saccharomyces cerevisiae*) the absorbances were determined in this part [44].

The study investigated the inhibitory effect of a natural molecule on α-amylase (α-Amylase gives from porcine pancreas, A3176-sigma Aldrich), employing the methodology outlined by Xiao et al. [45]. The starch solution used in this investigation was made by dissolving 6 µg of starch in 240 µL of NaOH and boiling it for 25 minutes at 70 °C. Also, the solution was also chilled in ice-cold water, the pH was adjusted to 6.9 with HCl, and 300 µL of water was added. 5 mg and 5 mL of EtOH:H_2O were combined

to create the sample solution. In the unlikely event that the enzyme was totally inhibited, we had several PB solutions ready. The substrate (50 µL), PB solution (pH 6.9, 100 µL), and sample (5-200 µL) solutions were mixed following a 30-minute pre-incubation at 37 °C. Next, 10 µL of a 50 g/mL enzyme solution was added. Thirty minutes were given to the solution to incubate. At 580 nm, the absorbances were determined using spectrophotometry [46].

Results and discussion

Enzymes results

Long-chain carbs in food are hydrolyzed by the small intestine's -glucosidase enzyme to produce monosaccharide units, which enter the bloodstream and cause hyperglycemia. Therefore, inhibiting α-glucosidase has emerged as a crucial therapeutic target that can delay the breakdown of carbohydrates and lower blood sugar levels. On the other hand, the -glucosidase inhibitors mainly target hyperglycemia without affecting insulin secretion [47]. Consequently, these are considered first-line oral sugar-lowering drugs and are used as monotherapy in the treatment of mild diabetic cases. In contrast, these are used in combination therapy with insulin or other medications in the event of acute diabetes complications. Acarbose, voglibose, and miglitol are the three α-glucosidase inhibitors that are now in use and available for purchase. Regretfully, studies have shown that these medications not only lack efficacy but also have a host of adverse effects, such as gas, bloating, diarrhea, and abdominal pain. These considerations prompted scientists to focus their efforts on finding new compounds, and many of these have been found as -glucosidase inhibitors in the last few years [48]. The investigated compound's IC50 values on the enzymes α-amylase and α-glucosidase were found to be 45.13 and 11.82 µM, respectively (Figure 1). The development of potent compounds that can inhibit -amylase activity and reduce blood sugar levels is a current area of research attention. There are two ways to obtain bioactive substances: through natural extraction and biosynthesis. N-acylhydrazone derivatives were tested as a potential novel anti-diabetic drug for biosynthesis because of their α-amylase inhibitory effect. It has been suggested that numerous chemical extracts from the plants *Rubus corchorifolius*, *Dalbergia odorifera*, and *Allmania nodiflora* could be used to create α-amylase inhibitors in natural extraction. Additionally, a characteristic class of naturally derived bioactive chemicals with hypoglycemic action is the flavonoid family. Plant-derived bioactive flavonoids have been shown to be able to limit the activity of α-amylase in several in vitro investigations, mostly because of their impacts on the its structure of enzymes [49].
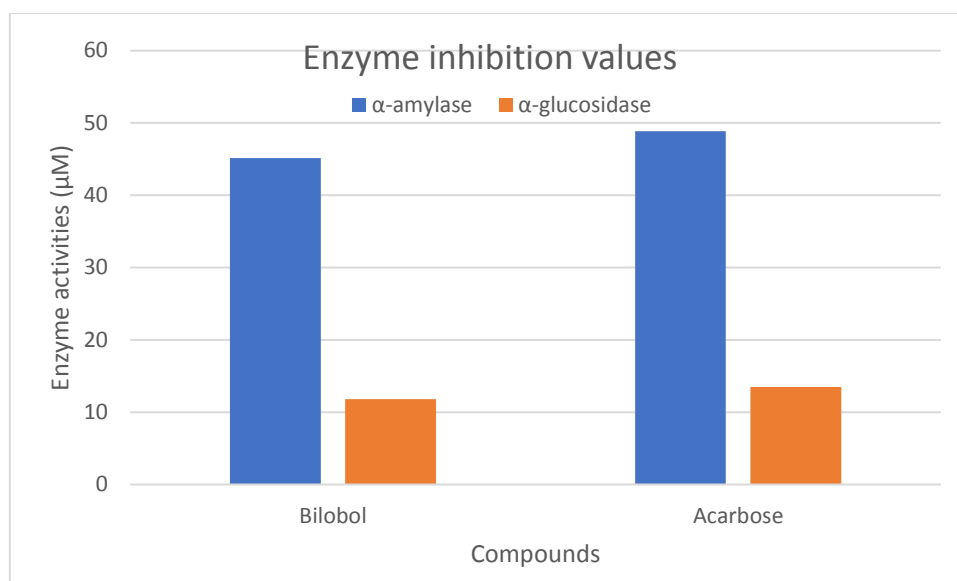
Figure 1. Enzymes results

Anti-breast cancer section

Plant extracts and natural compounds are effective medicines that have been determined to have antibacterial, antioxidant, anti-pulmonary fibrosis, and anti-inflammatory actions and may be reliable cancer treatment options. Recent studies suggest that plant extracts may include anticancer agents that have been proven to be effective against a variety of malignancies [50]. Antioxidant properties of bilobol appear to be responsible for the anti-human breast cancer impact against Hs578T, SkBr3, MDA-MB-231, BT-549, MCF-7, AU565, Evsa-T, and 600MPE breast cancer cells. The viability of cancer cell lines (MDA-MB-231, Hs578T, SkBr3, BT-549, MCF-7, AU565, Evsa-T, and 600MPE) reduced by Bilobol (Table 1). The Bilobol IC_{50} was 236, 258, 265, 161, 250, 183, 256, and 233 µg/mL against MDA-MB-231, SkBr3, Hs578T, MCF-7, Evsa-T, BT-549, AU565, and 600MPE, respectively (Table 1). Several reports indicate that bilobol may have anti-cancer properties against various malignancies. To the best of our knowledge, there hasn't been any research done to identify the pathways involved in bilobol activity, despite multiple studies examining the anti-cancer efficacy of this natural substance against breast cancer. This study intends to examine the molecular mechanisms behind bilobol's anti-cancer action against breast cancer [51-55]. The anticancer activity of Bilobol on MCF-7 cell line is more efficient.

Table 1. The IC50 of Bilobol in the anti-breast cancer test.

Cell lines	Bilobol (µg/mL)
SkBr3	258.65±12.98
MDA-MB-231	236.13±10.97
MCF-7	161.08±8.06
Hs578T	265.36±24.81
Evsa-T	250.28±13.66
BT-549	183.06±10.72
AU565	256.13±17.31
600MPE	233.64±11.84
HUVEC	312.89±19.52

Oxidation is a harmful process that alters chemical composition and depletes nutrients. Fats and oils are highly vulnerable to oxidation. Oils and fats get spicy due to oxidation. Furthermore, byproducts of lipid oxidation have the potential to damage other dietary ingredients [56–59]. Therefore, in addition to the harmful organoleptic effects of food products, they can also have a variety of side effects by poisoning the body and destroying vital vitamins and fatty acids. Because manufactured antioxidants are hazardous and consumers are accepting of natural additions, there is a growing demand to employ natural antioxidant molecules. These antioxidants, known as polyphenolic compounds, are found in every part of a plant, including the leaves, stems, fruits, roots, and seeds. [60]. Antioxidants found in fruits and vegetables are partially responsible for their ability to protect against chronic diseases. These days, a lot of research is done on the antioxidant qualities of natural antioxidants derived from plants and spices [61-63].

Molecular docking

Through the use of molecular modeling calculations, the chemical activities of bilobol were assessed with the enzymes (alpha amylase and alpha-glucosidase) and proteins (CD47, EGFR, androgen receptor, folate receptor, progesterone receptor, CD44, HER2, and estrogen receptor). The results indicated the likely biomolecule residues that could forge potent connections with this substance. Figure 2A displays the docking position of bilobol amid the alpha amylase residues. Figure 2B shows how bilobol and alpha amylase interact with one another. As demonstrated in Fig. 2B, bilobol has formed two hydrogen bonds with the alpha amylase residues. They are Asp300 and Glu233 residues. The hydrophobic interaction is one of the additional interactions that raises bilobol's affinity for binding to the enzyme. The remaining residues that exhibit hydrophobic interaction include Tyr62, Ala106, Val107, Leu162, Leu165, and Ala195. Figure 3A depicts the modeling position of bilobol among the alpha glucosidase residues, whereas Figure 3B shows the interactions among them. Three hydrogen bonds have been formed between bilobol and alpha glucosidase. The residues in question are Glu856,

Ile823, and His 708. Table 2 displays the length of these hydrogen bonds. Other interactions that this chemical has produced include a hydrophobic interaction with alpha glucosidase residues Leu7112, Ala719, Ala749, Tyr822, Ile824, Pro825, and Leu857. The docking position of bilobol amid the CD47 residues is displayed in Fig. 4A. Fig. 4B shows the interactions between CD47 and bilobol. The molecule and the Lys43 and Thr91 residues of CD47 are joined by 2 H bonds. Additionally, this molecule has some hydrophobic interactions with Tyr113, Val115, Phe14, Phe42, and Val88 residues.

Figure 5A depicts the bilobol's docking position among the EGFR residues, whereas Figure 5B depicts their interactions. Bilobol not only exhibited new interactions, such as hydrophobic contacts with EGFR residues, but also produced two hydrogen bonds. The residues Leu38 and Pro248 have hydrogen bonds in them. The compound and residues Val36, Val37, Leu38, Ala62, Cys224, Leu225, Val226, Cys227, Ala234, Cys236, Pro248, Tyr251, and Ala265 form the hydrophobic interactions. Figure 6A depicts the position at which bilobol docks with the androgen receptor residues, whereas Figure 6B illustrates their interaction. Bilobol has created 2 H bonds with the residues of the androgen receptor. They are Lys808 and Glu681 residues. Additional interactions between this chemical and androgen receptor residues have been observed. Receptor residues and bilobol have eighteen hydrophobic interactions. Figure 7A depicts the bilobol's docking stance amid the folate receptor residues, whereas Figure 7B depicts the interactions. There are 2 H bonds among the folate receptor and bilobol. These residues are His135 and Asp81. Furthermore, this molecule and the folate receptor residues engage in two Pi-Pi stacking interactions. The specifics and type of created interactions between the chemical and receptor are depicted in Figure 7B.

Figure 8A shows the modeling position of bilobol amid the progesterone receptor residues. Figure 8B depicts their interactions. The findings show that two hydrogen bonds have been formed by bilobol with the residues Ile699 and Gln725. Also, the interactions exist as well, such as hydrophobic contacts among receptor residues and bilobol. Hydrophobic interactions are found in the residues Met692, Pro696, Val698, Val729, Trp732, and Trp765. Figure 9A shows the bilobol's docking position among the CD44 residues, while Figure 9B shows the interactions between those residues. Between the CD44 residues and Bilobol, 2 H bonds have been formed. Ile26 and Glu37 are these residues. Additionally, this molecule has some hydrophobic interactions with residues Tyr42, Cys77, Ile96, and Cys97. Figure 10A displays the bilobol's modeling position among the HER2 residues, whereas Figure 10B displays their interactions. The outcomes demonstrate that two hydrogen bonds between bilobol and the HER2 residues have been formed. Thr7 and Gly417 are these residues. Additionally, eight residues have formed hydrophobic bonds with bilobol. Phe236, Phe269, Tyr281, Cys289, Leu291, Leu414, and Ala418 are the residues in question. Figure 11A shows the docking position of bilobol amid the estrogen receptor residues. The compound's interactions with the receptor residues are discussed in Figure 11B. Bilobol and the estrogen receptor residues do not form hydrogen bonds. Other types of interactions do exist, though, such as hydrophobic contacts between bilobol and residues Leu539, Met543, Pro535,

Val355, and Leu354. In addition to describing possible interactions between chemical compounds and biomolecules, the molecular docking study can provide the binding affinity of the ligands to the biomolecules. This affinity can be shown in the docking score. For the ligand-protein and ligand-enzyme complexes that were previously reported, this value is displayed in Table 2. Even if bilobol is a useful inhibitor molecule against certain of these cancer cells and enzymes, it still needs to reach the target area. Vesicular nanocarriers are a suitable remedy for this problem, as they intensify their effects [64,65].
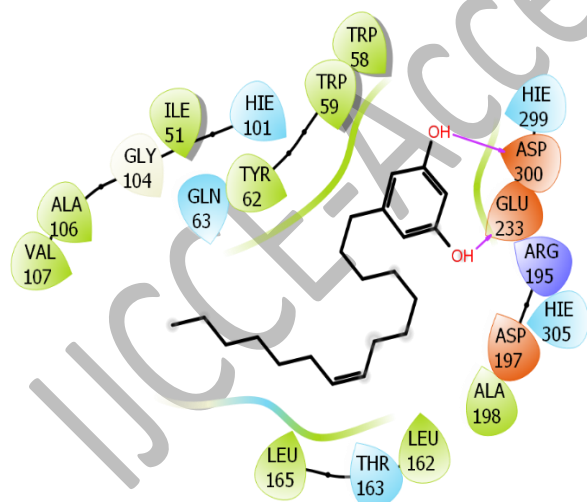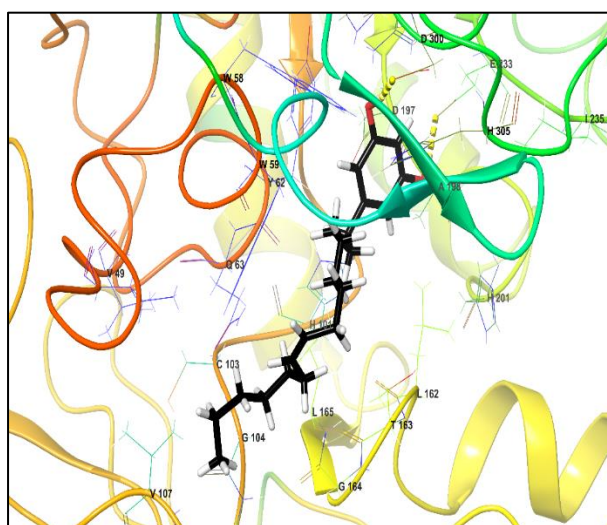
A   **B**

Figure 2. A) The Bilobol docking position in alpha amylase. B) The way that alpha amylase and bilobol interact. Purpole lines show the H-bonds that have been formed between the ligand and the enzyme.
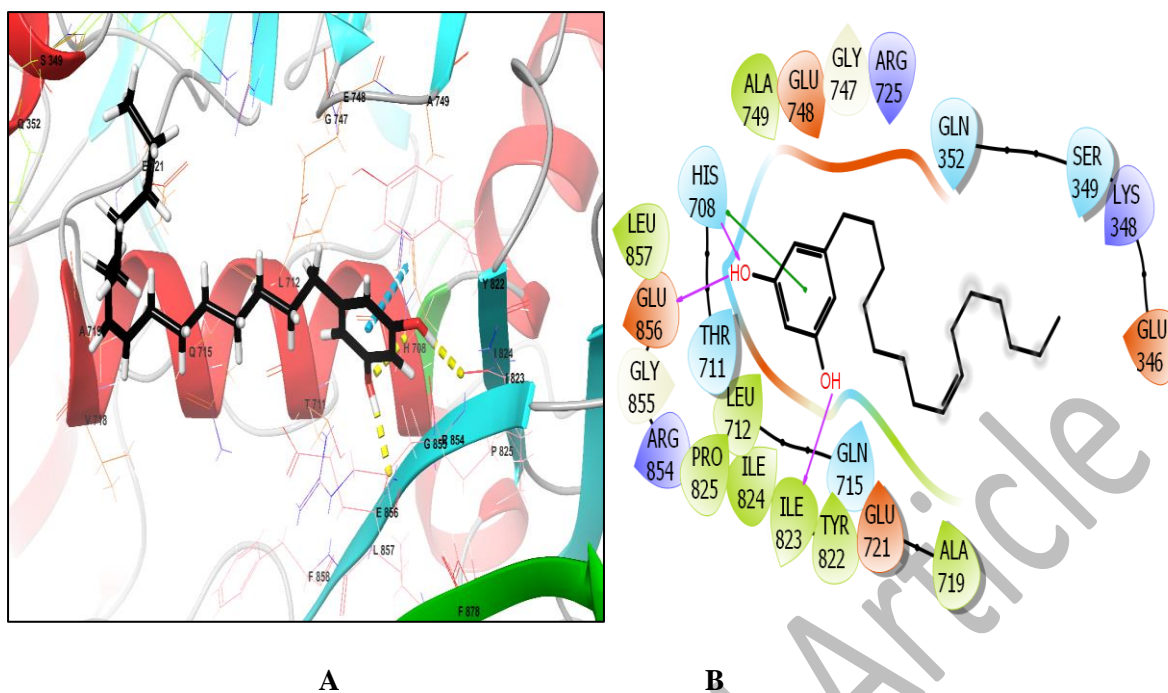
Figure 3. A) Bilobol's docking position with alpha glucosidase. B) Bilobol and alpha glucosidase interactions. The green line depicts the Pi-Pi stacking interaction, whereas the purple lines represent the hydrogen bonds.
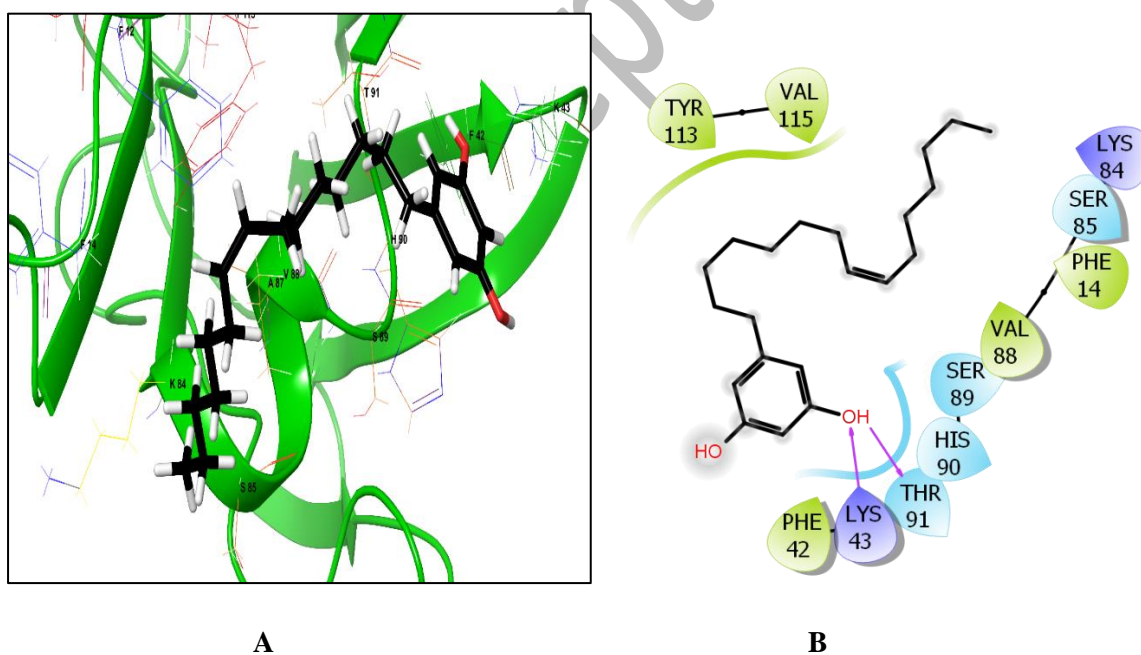
Figure 4. A) Bilobol's docking position among the residues of CD47. B) The way CD47 and bilobol interact. The formed H-bonds between the ligand and enzyme are shown by the purple lines.
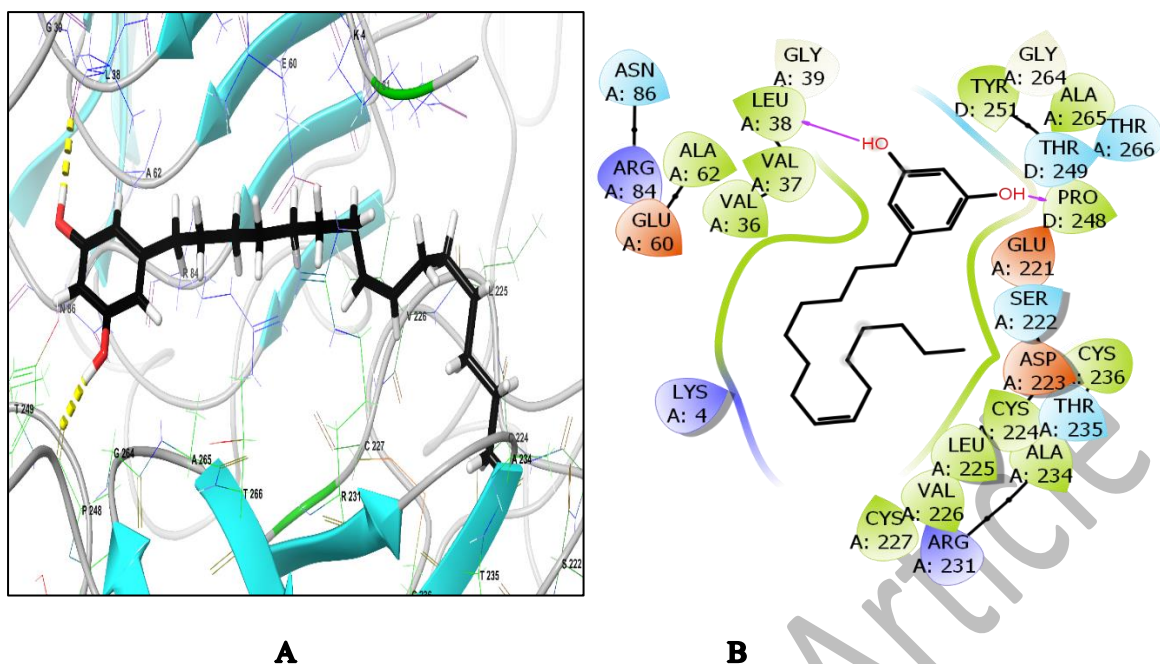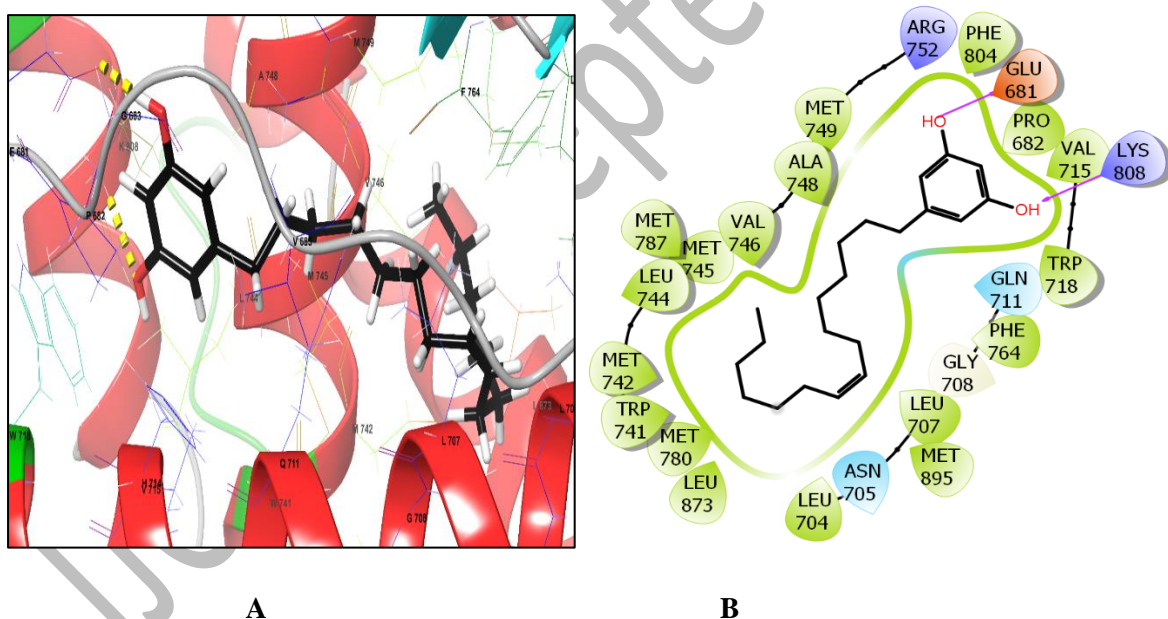
Figure 5. A) Bilobol's docking position among the EGFR residues. B) The way EGFR and bilobol interact. The formed H-bonds between the ligand and enzyme are shown by the purple lines.

Figure 6. A) Bilobol's docking position between androgen receptor residues. B) Bilobol and androgen receptor interactions. The formed H-bonds between the protein and ligand are shown by the purple lines.
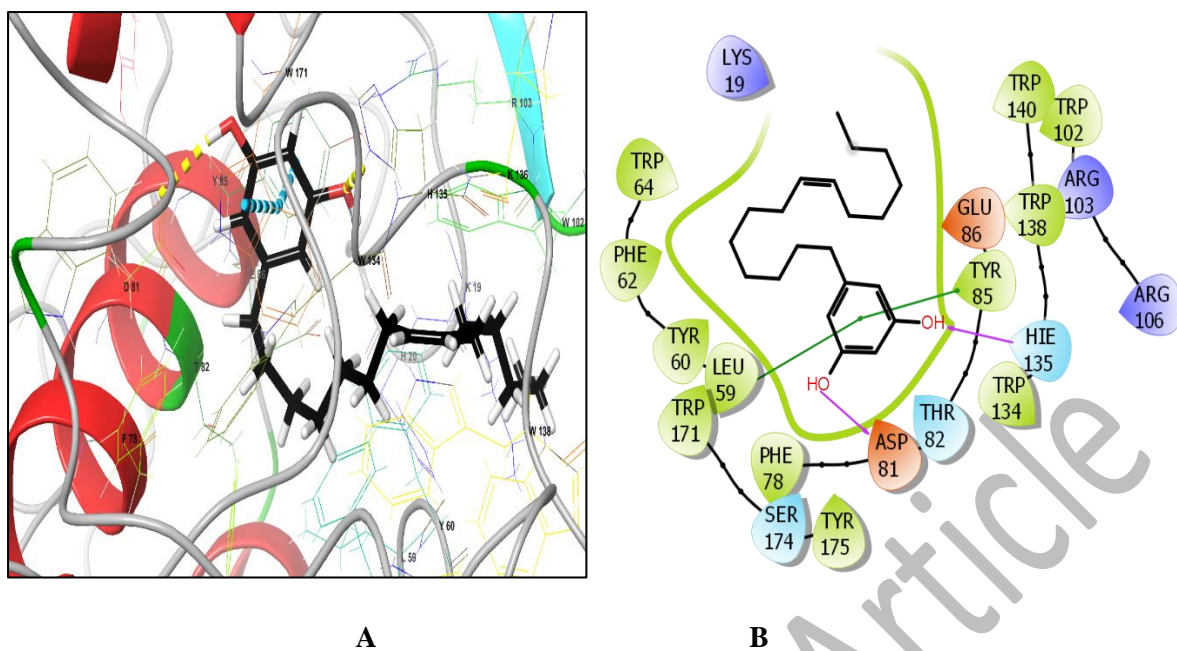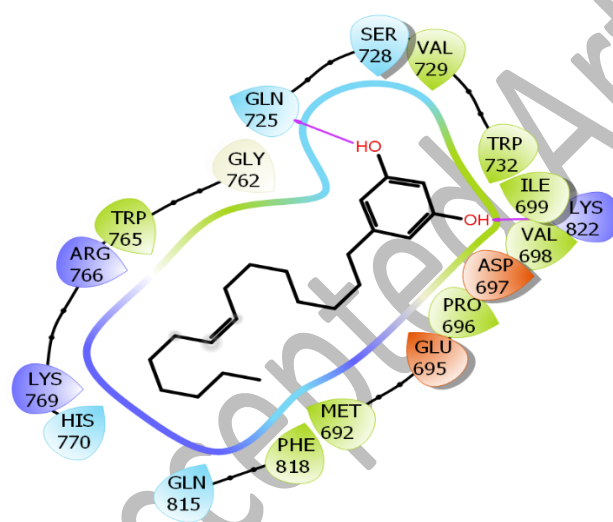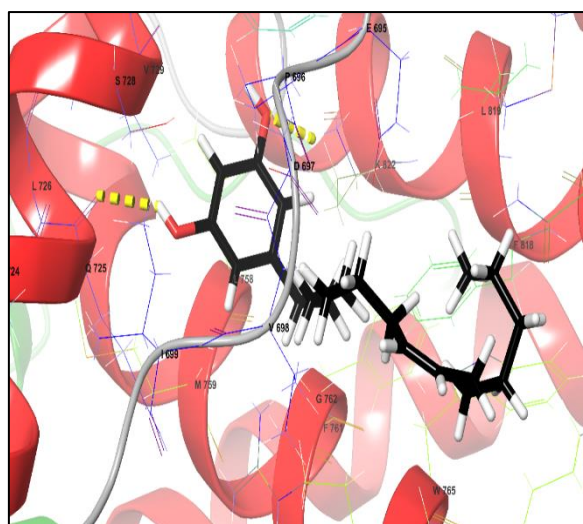
Figure 7. A) Bilobol's docking position amid the residues of the folate receptor. B) Bilobol and folate receptor interactions. Green lines depict the Pi-Pi stacking interaction between the protein and ligand, and purple lines represent the formed H-bonds.
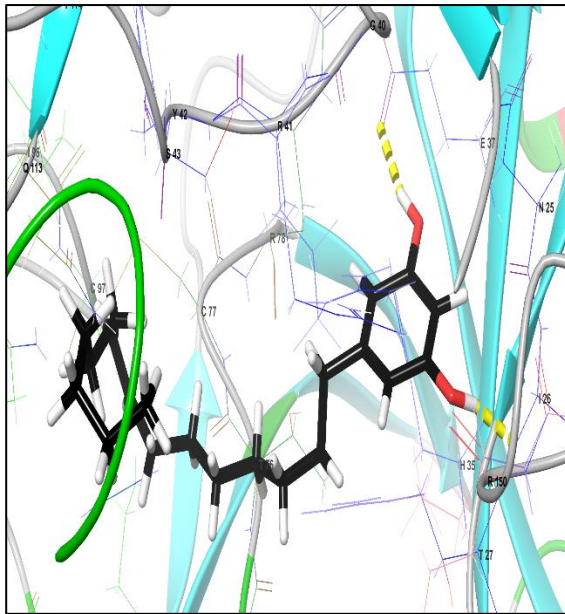
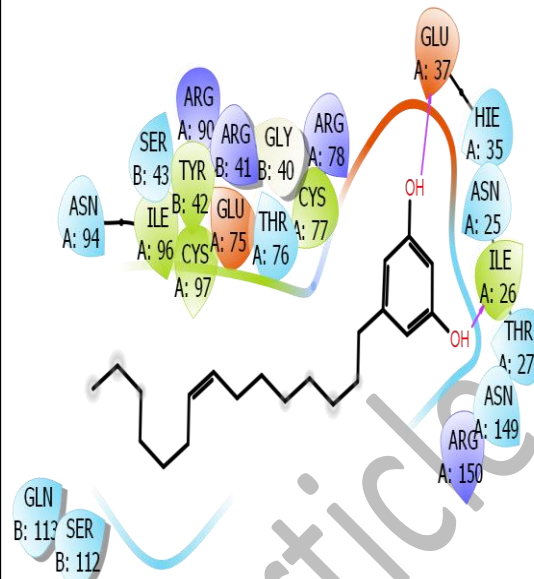**A**   **B**

Figure 8. A) Bilobol's position during docking among progestron receptor residues. B) Bilobol and progestron receptor interactions. The formed H-bonds between the protein and ligand are shown by the purple lines.
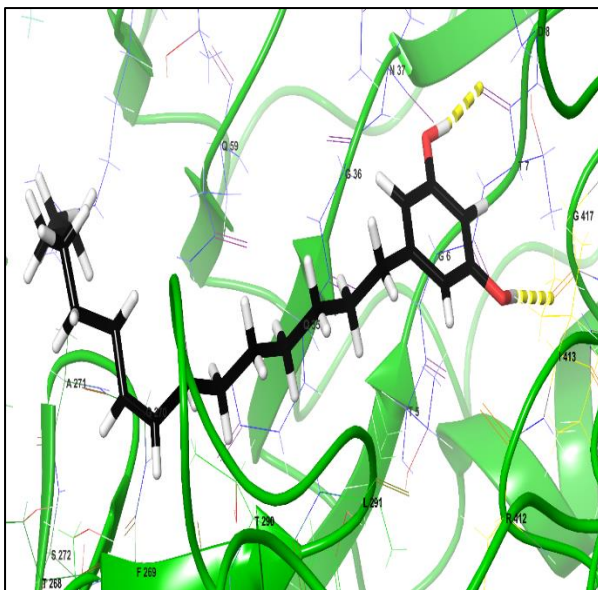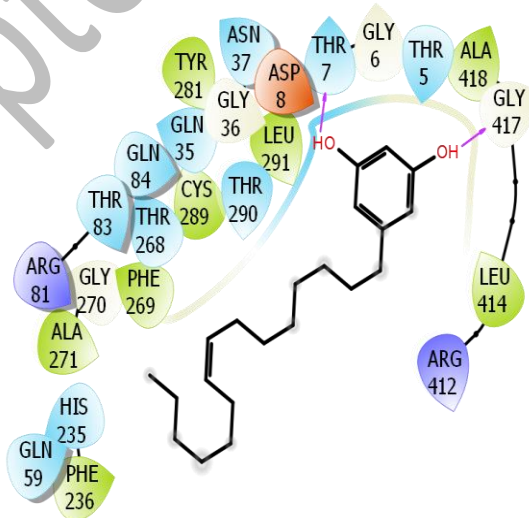
Figure 9. A) Bilobol's docking position among CD44 residues. B) The interactions of Bilobol with CD44. The formed H-bonds between the protein and ligand are shown by the purple lines.
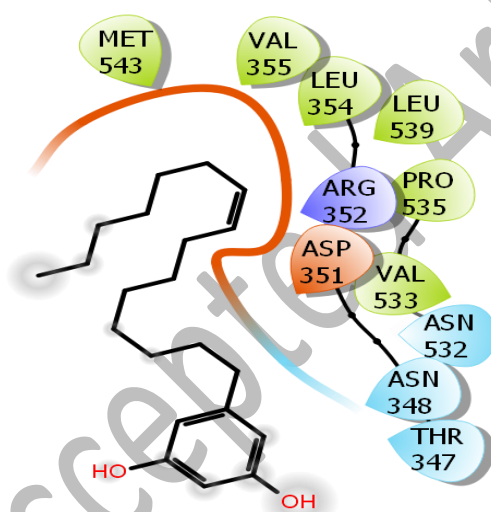

Figure 10. A) Bilobol's docking position among the HER2 residues. B) The way HER2 and Bilobol interact. The formed H-bonds between the protein and ligand are shown by the purple lines.
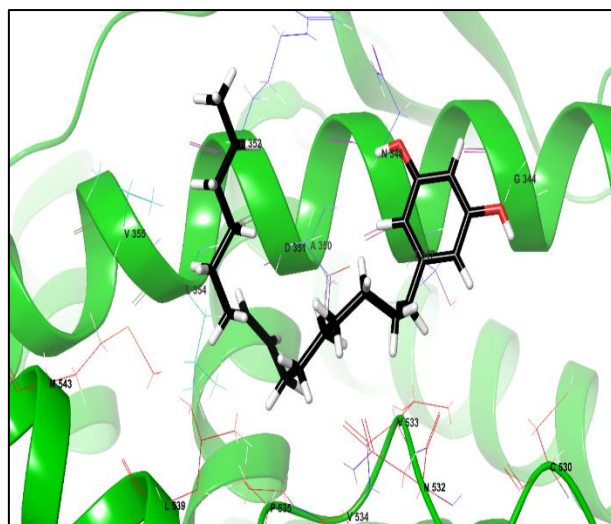
A   **B**

Figure 11. A) Bilobol's docking position amid the residues of estrogen receptors. B) Bilobol and estrogen receptor interactions. The formed H-bonds between the protein and ligand are shown by the purple lines.

Table 2. The molecular docking computations for enzymes and surface receptors yielded the following results: docking scores, residues containing H-bonds, and H-bond length.

Parameter	Docking score (kcal/mol)	Residues with H-bond and their length
Alpha amylase	-4.538	Glu233:1.83Å Asp300:1.81Å
Alpha glucosidase	-4.460	His708: 2.24Å Ile823: 1.65Å Glu856: 1.84Å
CD47 (SkBr3)	-2.063	Lys43: 2.51Å Thr91: 1.99Å
EGFR (MDA-MB-231)	-5.274	Leu38: 1.79Å Pro248: 1.65Å
Androgen receptor (MCF-7)	-3.70	Glu681: 1.65Å Lys808: 2.08Å
Folate receptor (Hs578T)	-8.582	Asp81: 2.27Å His135: 1.95Å
Progesterone receptor (Evsa-T)	-3.308	Met692: 2.09Å Gln725: 2.36Å
CD44 (BT-549)	-1.897	Ile26: 1.72Å Glu37: 1.92Å
HER2 (AU565)	-4.577	Thr7: 1.92Å Gly417: 2.11Å
Estrogen receptor (600MPE)	-1.737	_

CONCLUSIONS

Using MDA-MB-231, Hs578T, SkBr3, BT-549, MCF-7, AU565, Evsa-T, and 600MPE as test cancer cells, the cytotoxic and anticancer effects of bilobol were evaluated. The presence of bilobol reduced the viability of breast cancer cells. As useful tools for interpreting the findings of empirical research, in silico investigations could be carried out. From a more specialized standpoint, these methods can shed light on the interactions. One technology that has attracted the most attention is molecular docking, which can define possible interactions between biomolecules and ligands at the atomic level. The effectiveness of bilobol's inhibition of alpha-glucosidase and alpha-amylase and activity was assessed in this work using molecular docking. In the breast cancer cell lines Hs578T, MDA-MB-231, SkBr3, BT-549, MCF-7, AU565, 600MPE, and Evsa-T, Eight surface receptor proteins that are expressed were tested for this compound's activities: CD47, EGFR, androgen receptor, folate receptor, progesterone

receptor, CD44, HER2, and estrogen receptor. The findings indicated that bilobol might be regarded as a possible inhibitor for the cancer cell lines and the aforementioned enzymes.

Data Availability Statement

The data that support the findings of this study are available from the corresponding author upon reasonable request.

Conflict of interest statement

The authors declare that there are no conflicts of interest.

References

[1] Xu, J., Li, Y., Yang, X., Liu, Y., Chen, Y., & Chen, M. Bilobol inhibits the lipopolysaccharide-induced expression and distribution of RhoA in HepG2 human hepatocellular carcinoma cells. *Oncol. Lett.*, **10(2)**: 962-966 (2015).

[2] Elkhenany, H., Abd Elkodous, M., Ghoneim, N. I., Ahmed, T. A., Ahmed, S. M., Mohamed, I. K., & El-Badri, N. Comparison of different uncoated and starch-coated superparamagnetic iron oxide nanoparticles: implications for stem cell tracking. *Int. J. Biol. Macromol*, **143**: 763-774 (2020).

[3] Borm, P.J., Robbins, D., and Haubold, S. The potential risks of nanomaterials: a review carried out for ECETOC. *Part Fibre Toxicol*. **3(1)**: 11 (2006).

[4] Stapleton, P.A., and Nurkiewicz, T.R., 2014. Vascular distribution of nanomaterials. *Wiley Interdiscip Rev Nanomed Nanobiotechnol.* **6(4)**: 338-348 (2014).

[5] Patra, J.K., Das, G., Faceto, L.F., Campos, E.V.R., and Rodriguez-Torres, M.D.P., Acosta-Torres, L.S., DiazTorres, L.A., Grillo, R., Swamy, M.K., Sharma, S. Nano based drug delivery systems: Recent developments and future prospects. *J. Nanobiotechnology*. **16**: 71 (2018).

[6] Itani, R., and Al Faraj, S.A. siRNA Conjugated Nanoparticles-A Next Generation Strategy to Treat Lung Cancer. *Int. J. Mol. Sci*. **20**(23): 6088 (2019).

[7] Trojer, M.A., Li, Y., Wallin, M., Holmberg, K. and Nyden, M. Charged microcapsules for controlled release of hydrophobic actives Part II: surface modification by Lbl adsorption and lipid bilayer formation on properly anchored dispersant layers. *J. Colloid Interface Sci*. **409**: 8-17 (2013).

[8] Liu, D., Chen, L. and Jiang, S. Formulation and characterization of hydrophilic drug diclofenac sodium-loaded solid lipid nanoparticles based on phospholipid complexes technology. *J. Liposome Res*, **24**(1): 17-26 (2014).

[9] Koyyati, R., Kudle, K.R., Padigya, P.R.M., 2016. Evaluation of antibacterial and cytotoxic activity of green synthesized cobalt nanoparticles using Raphanus sativus var. longipinnatus leaf extract. *Int. J. Pharmtech Res*, **9(3)**: 466-72 (2016).

[10] Lu, Y., Wan, X., Li, L., Sun, P. and Liu, G. 2021. Synthesis of a reusable composite of graphene and silver nanoparticles for catalytic reduction of 4- nitrophenol and performance as anti-colorectal carcinoma. *J. Mater. Res. Technol*, **12:**1832-1843 (2021).

[11] Onwudiwe, D. C., Ravele, M. P. and Elemike, E. E. Eco-friendly synthesis, structural properties and morphology of cobalt hydroxide and cobalt oxide nanoparticles using extract of Litchi chinensis. *Nano-Struct. Nano-Objects*, **23**: 100470 (2020).

[12] Mihăşan, M. "What in silico molecular docking can do for the 'bench-working biologists,'" *J. Biosci*, **37**: 1089–1095, (2012).

[13] Poustforoosh, A., Hashemipour, H., Pardakhty, A., & Pour, M. K. Preparation of nano-micelles of meloxicam for transdermal drug delivery and simulation of drug release: A computational supported experimental study. *Can. J. Chem. Eng*, **100**(11): 3428-3436 (2022).

[14] Chandrika, B. R., Subramanian, J., & Sharma, S. D. Managing protein flexibility in docking and its applications. *Drug Discov. Today*, **14**: 394-400 (2009).

[15] Meng, X. Y., Zhang, H. X., Mezei, M., & Cui, M. Molecular docking: a powerful approach for structure-based drug discovery. *Curr comput-aid drug*, **7**(2): 146-157 (2011).

[16] Cardullo, N., Vera M., Luana P., Anaëlle C., Laurent P., Denis D., Stéphane Q., and Corrado T. "C-glucosidic ellagitannins and galloylated glucoses as potential functional food ingredients with anti-diabetic properties: A study of α-glucosidase and α-amylase inhibition." *Food chem*. **313**: 126099 (2020).

[17] Li, S., Weimin Z., Ruimin W., Congfa L., Xue L., and Lu W. "Screening and identification of natural α-glucosidase and α-amylase inhibitors from partridge tea (Mallotus furetianus Muell-Arg) and in silico analysis." *Food Chem*. **388**: 133004 (2022).

[18] Benayad, O., Bouhrim, M., Tiji, S., Kharchoufa, L., Addi, M., Drouet, S., Hano, C., Lorenzo, J.M., Bendaha, H., Bnouham, M. and Mimouni, M. Phytochemical profile, α-glucosidase, and α-

amylase inhibition potential and toxicity evaluation of extracts from Citrus aurantium (L) peel, a valuable by-product from Northeastern Morocco. *Biomolecules*, **11**(11): 1555 (2021).

[19] Saddique, F. A., Matloob A., Usman A. A., Muhammad M., Sadia S., and Magdi E.A.Z.. "Identification of cyclic sulfonamides with an N-arylacetamide group as α-glucosidase and α-amylase inhibitors: Biological evaluation and molecular modeling." *Pharmaceuticals* **15**: 106 (2022).

[20] Naghiyev, F., Mamedov, I., Askerov, R., Taslimi, P., & Poustforoosh, A. (2022). Synthesis and biological activity of functionally substituted pyrimidine and pyran derivatives on the basis of isatylidene malononitriles. *ChemistrySelect*, 7(33): e202202006 (2022).

[21] Mehrabani, M. et al., "Evaluation of the cytotoxicity, antibacterial, antioxidant, and anti-inflammatory effects of different extracts of Punica Granatum var. Pleniflora," *J. Kerman Univ. Med. Sci.*, **27**: 414–425 (2020).

[22] Hatherley, D., Graham, S. C., Turner, J., Harlos, K., Stuart, D. I., and Barclay, A. N. "Paired Receptor Specificity Explained by Structures of Signal Regulatory Proteins Alone and Complexed with CD47," *Molecular Cell*, **31**: 266–277, (2008).

[23] Menck, K. et al., "Characterisation of tumour-derived microvesicles in cancer patients' blood and correlation with clinical outcome," *J. Extracell. Vesicles*, **6**: 1, (2017).

[24] Freed, D. M. et al., "EGFR Ligands Differentially Stabilize Receptor Dimers to Specify Signaling Kinetics," *Cell*, **171**: 683-695 (2017).

[25] Price, J. T., Tiganis, T., Agarwal, A., Djakiew, D., and Thompson, E. W. "Epidermal growth factor promotes MDA-MB-231 breast cancer cell migration through a phosphatidylinositol 3'-kinase and phospholipase C-dependent mechanism," *Cancer Res.*, **59**: 5475–5478 (1999).

[26] Amicis, F. De. et al., "AIB1 sequestration by androgen receptor inhibits estrogen-dependent cyclin D1 expression in breast cancer cells," *BMC Cancer*, **19**: 1038, (2019).

[27] Hazhir, N., Chekin, F., Raoof, J. B., & Fathi, S. (2021). Anticancer activity of Doxorubicin conjugated to polymer/carbon based-nanohybrid against MCF-7 breast and HT-29 colon cancer cells. *Int J Nano Dimens*, **12**(1): 11-19 (2021).

[28] Vatandost, E., Saraei, A. G. H., Chekin, F., Raeisi, S. N., & Shahidi, S. A. Antioxidant, antibacterial and anticancer performance of reduced graphene oxide prepared via green tea extract assisted biosynthesis. ChemistrySelect, 5(33), 10401-10406 (2020).

[29] Necela, B. M., et al., "Folate Receptor-α (FOLR1) Expression and Function in Triple Negative Tumors," PLOS ONE, **10**: e0122209, (2015).

[30] Borras, M., Lacroix, M., Legros, N., and Leclercq, G. "Estrogen receptor-negative/progesterone receptor-positive Evsa-T mammary tumor cells: A model for assessing the biological property of this peculiar phenotype of breast cancers," *Cancer Letters*, 120: 23–30, (1997).

[31] Liu, L. K., and Finzel, B. "High-resolution crystal structures of alternate forms of the human CD44 hyaluronan-binding domain reveal a site for protein interaction," *Acta Crystallogr. F:Struct. Biol*, **70**: 1155–1161, (2014).

[32] Hu, S. et al., "CD44 cross-linking increases malignancy of breast cancer via upregulation of p-Moesin," *Cancer Cell International*, 20: 563, (2020).

[33] Wang, C. et al., "The Synergistic Effects of Pyrotinib Combined With Adriamycin on HER2-Positive Breast Cancer," *Frontiers in Oncology*, 11: (2021).

[34] Mora, R., Vidal et al., "Epidermal Growth Factor Receptor Family Inhibition Identifies P38 Mitogen-activated Protein Kinase as a Potential Therapeutic Target in Bladder Cancer," *Urology*, **112**: 225.e1-225.e7, (2018).

[35] Dai, X., Cheng, H., Bai, Z., J. Li, J. "Breast cancer cell line classification and Its relevance with breast tumor subtyping," *J Cancer*, 8: 3131–3141, (2017).

[36] Poustforoosh, A., Faramarz, S., Nematollahi, M.H., Hashemipour, H., Negahdaripour, M., and Pardakhty, A. "In silico SELEX screening and statistical analysis of newly designed 5mer peptide-aptamers as Bcl-xl inhibitors using the Taguchi method," *Comput. Biol. Med*, **146**: 105632, (2022).

[37] Poustforoosh, A., Farmarz, S., Nematollahi, M.H., Hashemipour, H., and Pardakhty, A. "Construction of Bio-conjugated nano-vesicles using non-ionic surfactants for targeted drug delivery: A computational supported experimental study," *J. Mol. Liq*, **367**: 120588, (2022).

[38] Poustforoosh, A., Faramarz, S., et al, "Tracing the pathways and mechanisms involved in the anti-breast cancer activity of glycyrrhizin using bioinformatics tools and computational methods," *J. Biomol. Struct. Dyn*, 1–15, (2023).

[39] Poustforoosh, A., Faramarz, S., Negahdaripour, M., and Hashemipour, H. "Modeling and affinity maturation of an anti-CD20 nanobody: a comprehensive in-silico investigation," *Sci. Rep*, **13**: 582, (2023).

[40] Poustforoosh, A., Hashemipour, H., et al, "Evaluation of potential anti-RNA-dependent RNA polymerase (RdRP) drugs against the newly emerged model of COVID-19 RdRP using computational methods," *Biophys. Chem*, **272**: 106564, (2021).

[41] Poustforoosh, A. et al., "The Impact of D614G Mutation of SARS-COV-2 on the Efficacy of Anti-viral Drugs: A Comparative Molecular Docking and Molecular Dynamics Study," *Curr. Microbiol*, **79**: 241, (2022).

[42] Poustforoosh, A. et al., "3D-QSAR, molecular docking, molecular dynamics, and ADME/T analysis of marketed and newly designed flavonoids as inhibitors of Bcl-2 family proteins for targeting U-87 glioblastoma," *J. Cell. Biochem*, (2021).

[43] Tao, Y., Zhang, Y., Cheng, Y., Wang, Y. Rapid screening and identification of glucosidase inhibitors from mulberry leaves using enzyme-immobilized magnetic beads coupled with HPLC/MS and NMR. *Biomed. Chromatogr*., **27**: 148-155 (2013).

[44] Tavaf, Z., Dangolani, S. K., Yousefi, R., Panahi, F., Shahsavani, M. B., & Khalafi-Nezhad, A. Synthesis of new curcumin derivatives as influential antidiabetic α-glucosidase and α-amylase inhibitors with anti-oxidant activity. *Carbohydrate Res*, **494**: 108069 (2020).

[45] Xiao, Z., Storms, R., Tsang. A. quantitative starch-iodine method for measuring alpha-amylase and glucoamylase activities. *Anal. Biochem*., **351**: 146-148 (2006).

[46] Nguelefack, T. B., Christian K. F., Elvine P. N., and Adeline K. W. "Multimodal α-glucosidase and α-amylase inhibition and antioxidant effect of the aqueous and methanol extracts from the trunk bark of Ceiba pentandra." *BioMed research international* **2020**: (2020).

[47] Singh, P., Serisha M., Nagaraju K., Ashona S., Lalitha G., Ochuko L. E., and Md Shahidul I. "Comparative α-glucosidase and α-amylase inhibition studies of rhodanine–pyrazole conjugates and their simple rhodanine analogues." *Med Chem Res* **28**: 143-159 (2019).

[48] El Sayed, H., et al. "New 4-(arylidene) amino-1, 2, 4-traizole-5-thiol derivatives and their acyclo thioglycosides as α-glucosidase and α-amylase inhibitors: Design, synthesis, and molecular modelling studies." *J Mol Struct* **1259**: 132733 (2022).

[49] Figueiredo-González, M., et al. "The involvement of phenolic-rich extracts from Galician autochthonous extra-virgin olive oils against the α-glucosidase and α-amylase inhibition." *Int. Food Res. J.* **116**: 447-454 (2019).

[50] Ma, L., et al. Introducing a novel chemotherapeutic drug formulated by iron nanoparticles for the clinical trial studies. *Appl. Organomet. Chem*, **36**: e5498 (2022).

[51] Lademann, J., Richter, H., Teichmann, A., Otberg, N., Blume-Peytavi, U., Luengo, J., Weiss, B., Schaefer, U.F., Lehr, C.M., Wepf, R. and Sterry, W. Nanoparticles–an efficient carrier for drug delivery into the hair follicles. *Eur. J. Pharm. Biopharm*. **66**(2): 159–64 (2007).

[52] Manikala, V. Synthesis, Molecular Docking and Anticancer Activity of Novel (E)-5-((1-phenyl-1H-1, 2, 3-triazol-4-yl) methylene)-2-thioxothiazolidin-4-one Analogues. *Iran. J. Chem. Chem. Eng,* **40**: 1793-1799 (2021).

[53] Shahabi, J., Akbarzadeh, A., Heydari Nasab, A., & Ardjmand, M. Doxorubicin loaded liposomal nanoparticles containing quantum dot for treatment of breast cancer. *Iran. J. Chem. Chem. Eng,* **38**: 45-53 (2019).

[54] Altun, Z., Yoruç, Z., & Boz, M. Synthesis and Biological activity of a New Pt (II) Complex Involving 4-bromo-2, 6-bis-hydroxymethyl-phenol and Nicotinamide. *Iran. J. Chem. Chem. Eng*, **41**: 3233-3250 (2021).

[55] Zivdar, M., Salahvarzi, S., & Dadgar, Z. Derivatization of Curcumin and the Effect of Resultant Derivatives on BRC-9 Breast Cancer Cells. *Iran. J. Chem. Chem. Eng,* **41**: 1224-1231 (2022).

[56] Yu, H., Cheng, L., Yin, J., Yan, S., Liu, K., Zhang, F., Xu, B. and Li, L. Structure and physicochemical properties of starches in lotus (Nelumbo nucifera Gaertn.) rhizome. *Food Science. Nutr.* **1**(4): 273-283 (2013).

[57] Nagajyothi, P. C., Muthuraman, P., Sreekanth, T. V. M., Kim, D. H. and Shim, J., Green synthesis: in-vitro anticancer activity of copper oxide nanoparticles against human cervical carcinoma cells. *Arab. J. Chem.* **10**: 215-225 (2017).

[58] Namvar, F., Rahman, H.S., and Mohamad, R. Cytotoxic effect of magnetic iron oxide nanoparticles synthesized via seaweed aqueous extract. *Int J Nanomedicine*. **19**: 2479-88 (2014).

[59] Sankar, R., Maheswari, R. and Karthik, S. Anticancer activity of Ficus religiosa engineered copper oxide nanoparticles. *Mater. Sci. Eng. C*. **44**: 234-239 (2014).

[60] Yang, F., Jin, C., and Jiang, Y. Liposome based delivery systems in pancreatic cancer treatment: from bench to bedside. *Cancer Treat. Rev*. **37**: 633-642 (2011).

[61] Sangami, S., and Manu, M. Synthesis of Green Iron Nanoparticles using Laterite and their application as a Fenton-like catalyst for the degradation of herbicide Ametryn in water, *Environ. Technol. Innov*. **8**: 150–163 (2017).

[62] Katata-Seru, L., Moremedi, T. and Aremu, O.S. Green synthesis of iron nanoparticles using Moringa oleifera extracts and their applications: Removal of nitrate from water and antibacterial activity against Escherichia coli. *J. Mol. Liq*, **256**: 296-304 (2018).

[63] Radini, I.A., Hasan, N., and Malik, M.A. Biosynthesis of iron nanoparticles using Trigonella foenum-graecum seed extract for photocatalytic methyl orange dye degradation and antibacterial applications. *J. Photochem. Photobiol. B: Biol*. **183**: 154-163 (2018).

[64] Poustforoosh, A., Nematollahi, M.H., Hashemipour, H., and Pardakhty, A. "Recent advances in Bio-conjugated nanocarriers for crossing the Blood-Brain Barrier in (pre-)clinical studies with an emphasis on vesicles," *J Control Release*, **343**: 777–797, (2022).

[65] Asadikaram, G., Poustforoosh, A., Pardakhty, A., Torkzadeh-Mahani, M., Nematollahi, M.H. "Niosomal virosome derived by vesicular stomatitis virus glycoprotein as a new gene carrier," *Biochem Biophys Res Commun*, **534**: 980–987, (2020).